



# Enhanced Lubrication Ability of Polyalphaolefin and Polypropylene Glycol by COOH-Functionalized Multiwalled Carbon Nanotubes as an Additive

Homender Kumar and A.P. Harsha

Submitted: 12 June 2020 / Revised: 13 November 2020 / Accepted: 19 December 2020 / Published online: 8 January 2021

**In the current study, the tribological performance of two different synthetic lubricants, i.e., polyalphaolefin (PAO 100) and polypropylene glycol (PPG 2000), were analyzed. The COOH-functionalized multiwalled carbon nanotubes (MWCNTs) were used as an additive in varying fractions (0.025-0.15 wt. %). The friction and wear studies were carried out as per ASTM D6425 by using SRV 5 tribometer with a 'ball on disk' configuration. The results showed that tribological performance gets enhanced remarkably with the inclusion of MWCNTs in both lubricants as compared to the pure lubricants. PAO 100 demonstrated the lowest coefficient of friction and wear volume at a concentration of 0.025 and 0.05 wt. % of MWCNTs, respectively. However, 0.025 wt. % of additive in PPG 2000 exhibited the maximum reduction in the coefficient of friction (~6%) and wear volume (~86%). The results confirmed that PAO 100 showed better tribological performance as compared to PPG 2000. The lubrication mechanism of MWCNTs has been demonstrated through the investigation of worn steel ball surfaces by using various characterization techniques such as scanning electron microscope, energy-dispersive x-ray spectroscopy (EDS) and scan probe microscope.**

**Keywords** friction, multiwalled carbon nanotubes (MWCNTs), polyalphaolefins (PAO), polypropylene glycol (PPG), wear

## 1. Introduction

Carbon nanotubes (CNTs) have been the focus of much attention because of their excellent physical, mechanical, electrical and thermal properties (Ref 1). In recent years, CNTs have found many applications such as in superconductors, sensors (i.e., gas sensor, strain, pressure measurement, biosensors), electronic devices (antennas for radio, brushes for commercial electronic motor, very large system integration [VLSI] interconnect), energy storage (i.e., lithium battery anodes, supercapacitor, hydrogen storage) and field emission devices (i.e., field emission display, ionization gauge, x-ray gun), electromagnetic wave absorption and shielding and nanotube composites (by filling or coating) (Ref 2). The CNTs fall in the category of one-dimensional nanomaterials in contrast to other carbon nanomaterials (e.g., fullerene (zero-dimensional), graphene (two-dimensional), diamond and graphite (three-dimensional)) (Ref 3). Generally, CNTs are divided into two categories: single-walled carbon nanotubes (SWCNTs) and multiwalled carbon nanotubes (MWCNTs). SWCNTs appear in a single layer of graphene wrapped up cylindrically to form a hollow-type structure, whereas MWCNTs are the

combination of multiple layers of graphite that are bound coaxially around a cylinder with interlayer distance (Ref 4). Excellent mechanical properties and the tubular shape of CNTs enable them to sustain high loads in tribological applications and also be useful as a lubricant additive (Ref 5). One of the major drawbacks of CNTs is chemical inertness and high surface energy (Ref 6), which lead to poor dispersion or solubility in most of the solvents that restrict their applications (Ref 7). It was assumed that the modification in the surface chemistry of CNTs by the introduction of organic compounds (functional groups) could enhance tribological performance of lubricants (Ref 8) as well as a composite medium (Ref 9). Generically, the electrical and mechanical properties of SWCNTs can be altered when functionalized; as a result, structural imperfections are caused by C=C bond breakages during the chemical processes. Nevertheless, the elemental properties of CNTs can be maintained by the surface grafting of MWCNTs, where the outer wall of MWCNTs is treated for the chemical modification, resulting in their higher tensile strength than SWCNTs. In addition, because of low production cost and their availability in large quantities, MWCNTs prove to be more attractive than SWCNTs (Ref 10). Therefore, surface-modified MWCNTs have been investigated by the many researchers for numerous tribological applications as a lubricant additive in oil (Ref 8, 11-13) and water (Ref 5, 7, 14-17). The results revealed that chemical modification leads to an improvement in the dispersion stability of MWNTs as well as in the tribological properties of lubricants.

Polyalphaolefins (PAOs) are synthetic lubricants that are assigned to group IV by the American Petroleum Society (API). PAOs are generally categorized based on their kinematic viscosity at 100°C (Ref 18). They are saturated olefin polymers produced by the catalytic oligomerization of linear- $\alpha$ -olefin (normally 1-decene). PAOs offer various intrinsic properties such as high viscosity index, better oxidative and thermal

**Homender Kumar and A.P. Harsha**, Tribology Laboratory, Department of Mechanical Engineering, Indian Institute of Technology (Banaras Hindu University), Varanasi 221005, India. Contact e-mails: harshaap@gmail.com and aphaarsha.mec@itbhu.ac.in.

stability, low volatility, lower toxicity and use in a wide range of temperature (Ref 19). PAOs are extensively used in automatic transmission oil, hydraulic oil, automobile industry as engine lubricants and gear oil, turbine oil, compressor and pump oil and greases (Ref 18). In the last few years, many researchers investigated various nanoparticles as an additive in the different grades of PAOs and reported comparative friction and wear characteristics in the test results after adding nanolubricants (Ref 20-30). However, only a very few studies have investigated the addition of MWCNTs in PAOs (Ref 31, 32).

In many applications, high performance is necessary, requiring distinctive specifications that are not met by conventional petroleum-based lubricants and PAOs. One of the most versatile synthetic lubricants is polyalkylene glycol (PAG). PAGs are included in the category of group V lubricants by the American Petroleum Society (API). PAG oils are classified by their weight percentage composition of ethylene oxide versus propylene oxide units in the polymer chain. PAGs with 50-75 wt.% ethylene oxide are called polyethylene glycols (PEGs), which are water soluble, whereas PAGs with 100 wt.% propylene oxide groups are called polypropylene glycols (PPGs), which are water insoluble (Ref 33). PPG is a linear polymer manufactured from the downstream derivative of propylene oxide under controlled, catalyzed reaction of propylene oxide and water (Ref 19). PPGs are divided into two categories: low molecular weight PPGs (i.e., PPG 400, PPG 600 and PPG 750) and higher molecular weight PPGs (PPG 2000, PPG 3000, PPG 4000). Compared to the conventional mineral oils, PPG 2000 offers an excellent low and high-temperature characteristics, high viscosity indices, hydrolytic stability, excellent control of deposits and inherently superior lubricity, which may be further improved by the use of an additive (Ref 34, 35). The term 2000 indicates that the approximate average molecular weight is 2000. PPG 2000 has been broadly used as lubricant base stock in many industrial applications such as gear oil, compressor lubricants and hydraulic fluids. Tribological characteristics of aliphatic diols, with PEG and PPG as a lubricant between aluminum and steel, were studied using a FALEX tribometer by Igari et al. (Ref 36). It was found that wear in aluminum was reduced when alkyl groups were added to diols. Results from other research studies also demonstrate excellent lubricity of glycols (Ref 37, 38). However, no reports are available on the use of COOH-functionalized MWCNTs as an additive in the synthetic lubricants (i.e., PPG 2000).

In this investigation, COOH-functionalized MWCNTs are analyzed as a lubricant additive for two synthetic base oils of different viscosity index groups, i.e., polyalphaolefin (PAO 100) and polypropylene glycol (PPG 2000). The MWCNTs are dispersed in both base oil at varying concentrations of 0.025,

0.05, 0.075, 0.1 and 0.15 wt.% for the preparation of nanolubricants. The friction and wear properties have been studied as per ASTM D 6425 with the aid of a SRV 5 tribometer. The present study aims to investigate the effect of MWCNTs on the tribological performance of both lubricating oils and to compare their test results.

## 2. Experimental Details

### 2.1 Solid Lubricant Additive and Lubricants

The COOH-functionalized MWCNTs having an outer diameter 20-30 nm and length 1-2  $\mu\text{m}$  (manufacturer's data) were procured from Otto Chemie Pvt. Ltd., India. Polyalphaolefin (PAO 100) and polypropylene glycol (PPG 2000) were purchased from Synthomaxx India Pvt. Ltd., India. The typical properties of PAO 100 and PPG 2000 are listed in Table 1.

### 2.2 Nanolubricant Formulation

A varying concentration (0.025, 0.05, 0.075, 0.1 and 0.15 wt.%) of MWCNTs was blended in PAO 100 and PPG 2000 base oil with the help of magnetic stirrer. For the better dispersion of the additive in both oils, the blended solution was kept in ultrasonication bath for 1 h.

### 2.3 Tribological Testing

Tribological experimentation was performed by using SRV 5 tribometer (Optimol Instrument, Munich, Germany) in accordance with ASTM D6425 standard. Table 2 reports the test parameters and arrangement of the specimens. The ball on disk-type configuration was used in tribo-testing, which confirms the point contact between the mating surfaces at the beginning of tests. The initial Hertzian stress at the interface of the contact was around 3.14 GPa. Both the mating specimens were made from AISI 52100 high chromium-bearing steel. The diameter of the ball specimen was 10 mm, and microhardness was  $60 \pm 2$  HRC. The disk specimen had a thickness of  $7.85 \pm 0.1$  mm and diameter of  $24 \pm 0.5$  mm. The hardness was  $62 \pm 1$  HRC. In the test rig, the disk was mounted on a holder called the lower test specimen, while the test ball was loaded vertically with the aid of load rod, called as an upper test specimen. Before starting the experiments, 0.3 ml of lubricant was applied on the disk specimen at the contact area, which remained stationary throughout the test duration. The test ball oscillates against the disk with the assistance of oscillation drive rod. The coefficient of friction (COF) with respect to test duration was recorded in the computer through the data acquisition system, which is attached to the test rig. The

**Table 1 Physical properties of base oils (supplier's data)**

Property	PAO 100	PPG 2000
Kinematic viscosity (cSt@100°C), ASTM D445	100	24
Kinematic viscosity (cSt@40°C), ASTM D445	1150	160
Viscosity index, ASTM D2270	179	182
Density (g/ml), ASTM D1298	0.853	1.002
Pour point (°C), ASTM D97	-30	-30
Flash point (°C), ASTM D92	300	229

**Table 2 Summary of test parameters as per ASTM standards (D 6425)**

Parameters	Value
Configuration	Ball on disk
Test ball	52100 steel; Hardness: 60±2 HRC; Surface roughness: Ra 0.025µm ± 0.005; Diameter =10 mm
Disk	52100 steel; Hardness: 62±1 HRC; Surface roughness: 0.035µm < Ra < 0.050µm; Diameter =24 mm± 0.5 mm; Thickness =7.85 mm± 0.1 mm
Frequency (Hz)	50
Stroke (mm)	1
Temperature (°C)	80
Load (N)	300 N
Test duration (h)	2
Lubricant quantity (ml)	0.3
Environment	Laboratory air (Relative humidity 35-50%)

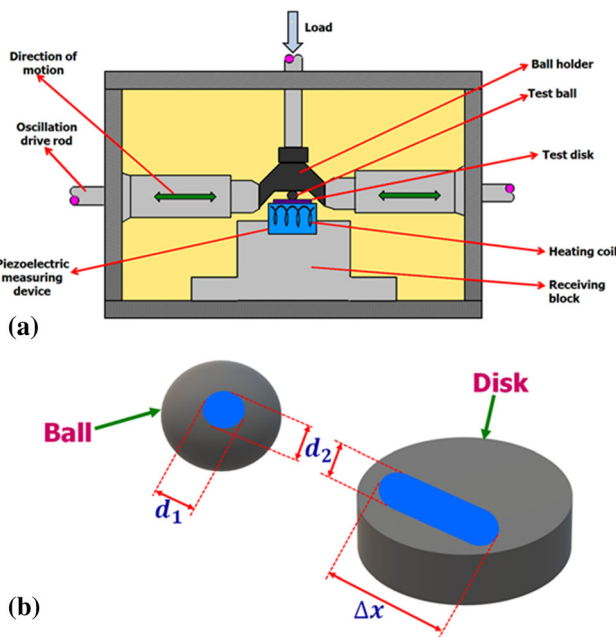


**Fig. 1** The schematic diagram of (a) SRV 5 test rig (b) wear scar of ball and disk and quantification of various parameters

schematic diagram of SRV 5 tribometer is portrayed in Fig. 1(a).

The wear volume of the ball on disk configuration was calculated by using Eq 1. Equations 2–6 are the auxiliary equations to Eq 1 (Ref 39).

$$W_V = W_{V_{ball}} + W_{V_{disk}} \quad (\text{Eq 1})$$

$$W_{V_{ball}} = \left( \frac{\pi W_{L_1} d_2^2}{8} \right) \quad (\text{Eq 2})$$

where

$$W_{L_1} = \left[ R - \left\{ \sqrt{\left( R^2 - \frac{d_2^2}{4} \right)} \right\} \right] - W_{L_2} \quad (\text{Eq 3})$$

$$W_{V_{disk}} = \left( \frac{\pi W_{L_2} d_2^2}{8} \right) + (\Delta x W_q) \quad (\text{Eq 4})$$

where

$$W_{L_2} = \left[ R' - \left\{ \sqrt{\left( R'^2 - \frac{d_2^2}{4} \right)} \right\} \right] \quad (\text{Eq 5})$$

$$R' = \frac{d_2^3}{12W_q} \quad (\text{Eq 6})$$

where  $d_2$  is wear scar diameter perpendicular to the sliding direction,  $R$  the radius of the ball,  $R'$  the approximate radius of wear scar on the disk after test,  $W_q$  the planimetric wear of the disk was measured by a profilometer,  $W_{L_1}$  and  $W_{L_2}$  the linear wear of ball and disk, respectively,  $W_{V_{ball}}$  and  $W_{V_{disk}}$  are volumetric wear of ball and disk, respectively, and  $\Delta x$  is the stroke length. The schematic diagram for the quantification of various parameters is shown in Fig. 1(b).

The film thickness and lubrication regime were calculated by presuming hard elastohydrodynamic lubrication (Ref 40), which is as given by Eq 7:

$$\frac{h_{min}}{R'} = 3.63 \left( \frac{u\eta_0}{E'R'} \right)^{0.68} (\xi E')^{0.49} \left( \frac{w}{E'R^2} \right)^{-0.073} (1 - e^{-0.68k}) \quad (\text{Eq 7})$$

where  $h_{min}$  is the minimum film thickness,  $u$  the mean velocity (m/s),  $\eta_0$  the dynamic viscosity of lubricant (PaS),  $E'$  the reduced Young's modulus (Pa),  $R'$  the reduced radius of curvature (m),  $\xi$  the pressure viscosity coefficient (m<sup>2</sup>/N) (Ref 41),  $w$  the normal load (N) and  $k$  the elliptical parameter.

The computed minimum film thickness for PAO 100 and PPG 2000 was 0.0916 µm and 0.0342 µm, respectively. The thickness ratio ( $\lambda = \frac{h_{min}}{\sigma^*}$ ) was estimated by using  $\sigma^*$  and  $h_{min}$ . The  $\sigma^*$  is the composite surface roughness (i.e.,  $\sigma^* = \sqrt{\sigma_1^2 + \sigma_2^2}$ ) where  $\sigma_1$  and  $\sigma_2$  are the surface roughness of the two-mating surfaces. The calculated  $\lambda$  value for PAO 100 and PPG 2000 was 2.22 and 0.831. It was observed that according to the theory of fundamentals of fluid film lubrication (Ref 42), the lubrication regime for PAO 100 was mixed or

partial lubrication. In contrast, it was boundary lubrication condition in the case of PPG 2000.

## 2.4 Characterization of MWCNTs and Worn Surfaces

The crystalline structure of MWCNTs was characterized by using x-ray diffractometer (XRD) with Cu-K $\alpha$  radiation in the range of 10°–90°. High-resolution transmission electron microscope (HR-TEM) was adopted to probe the morphological characteristics of the additive. Fourier transform infrared spectroscopy (FTIR) with scan rate of 40 cm<sup>-1</sup> in the spectrum range of 400–4000 cm<sup>-1</sup> was used for identification of functional groups on the surface of MWCNTs. To examine wear pattern and morphological analysis of the worn surface of the ball and disk, scanning electron microscope (SEM) was employed. The chemical elemental analysis of worn surfaces was carried out by using energy-dispersive x-ray spectroscopy (EDS), which is attached with SEM. The topography of worn surfaces was analyzed by a scan probe microscope (SPM).

## 3. Results and Discussion

### 3.1 Investigation of MWCNTs Stability in Base Oils

The stability of additives in the base oils is an essential parameter for ensuring the performance of nanolubricants. The stability of nanolubricants was examined by visual observation. The photographs of all nanolubricants at a varying concentration of MWCNTs were captured at different time periods, as shown in Fig. 2. In both base oils, no evidence of sedimentation was observed at all concentrations of MWCNTs even after four months. Figure 2(i) displays the in situ suspension mechanism and the role of the functional group. The hydrophilic segment of the functional group attached to the surface of MWCNTs and hydrophobic tail reacts with base oils. This phenomenon of modification of nanoadditive reduces the surface energy of MWCNTs, thereby enhancing the suspension stability of additives in the base oils for a longer period.

### 3.2 Characterization of COOH-Functionalized MWCNTs

The crystalline structure and phase identification of COOH-functionalized MWCNTs were examined by using XRD. The diffraction pattern of MWCNTs is shown in Fig. 3(a). The profile has a peak at an angle of 26.483°, 44.464°, 53.499° and 77.421°, which corresponds to (002), (100), (004) and (110) plane, respectively. All the peaks are identical to JCPDS reference code 00-008-0415 and show a graphitic hexagonal structure.

The FTIR spectra of functionalized MWCNTs are displayed in Fig. 3(b). A strong and broad peak was observed at 3442 cm<sup>-1</sup>. This peak was attributed to the vibration of the O-H group (Ref 43). The carbonyl group (C=O) was identified at 1717 cm<sup>-1</sup> (Ref 17). The results demonstrate that the COOH groups are successfully affixed on the surface of MWCNTs. The extra peaks at around 667 cm<sup>-1</sup> could be assigned to stretching vibration of C–O–C groups. The peak observed at 1576 cm<sup>-1</sup> is assigned to the stretching modes of aromatic C=C bond (Ref 5, 44, 45).

The nanostructure of MWCNTs was analyzed by HR-TEM examination. Low-resolution and high-resolution micrographs of HR-TEM are shown in Fig. 4(a) and (b). The low-resolution

image (Fig. 4(a)) revealed rod-type morphological characteristics and high-resolution image (Fig. 4(b)) displayed a hollow tubular structure of MWCNTs with 15 to 20 layers. With the help of IMAGE J software, the diameter of MWCNTs was measured. The variation in the outer diameter of MWCNTs with the number of counts is given in Fig. 4(c). The average outer diameter of the additive was observed to be ~ 20 nm, and the diameter distribution was in the range of 9 nm to 35 nm. Figure 4(d) displays the size vs. frequency distribution of MWCNTs, and most of the MWCNTs were in the range between 10 and 30 nm.

### 3.3 Friction and Wear Response of Nanolubricants

**3.3.1 Friction Performance of nanolubricants.** The variation in the average coefficient of friction (COF) and percentage attenuation with additive concentration for both base oils is shown in Fig. 5(a) and (b). The results demonstrated that incorporation of a small amount of additive in the base oils enhances COF to a significant level. In both nanolubricants, minimum coefficient of friction was achieved at 0.025 wt.% dose of the additive, and increasing concentration of the additive in both base oils above 0.025 wt.% leads to an increase in COF, but it remains lower than that of pure oil for PAO 100. In the case of PPG 2000 beyond 0.025 wt.% of MWCNTs, the increase in COF was higher relative to the base oil. This outcome may be caused by the aggregation of bundles of nanotubes, which initiates for three-body abrasion wear and it could be the reason for higher COF. At concentration of 0.025 wt.% of additive, the average COF for PAO 100 and PPG 2000 was 0.125 and 0.206, respectively, and maximum reduction in COF was 12 and 6%, respectively.

The variation of COF with time at concentration of 0.025 wt.% of MWCNTs as an additive in PAO 100 and PPG 2000 is presented in Fig. 5(c). For plain PAO 100, at the initial stage of the test, there was an increase in the COF and subsequently the variation of COF was almost independent of time. The rise in coefficient of friction at the initial stage may be due to the absence of film formation at the interface of mating pairs, which leads to a severe wear of surfaces as well as an increase in friction. The same trend is also seen for PAO 100 with 0.025 wt.% of the additive. While comparing the plain PAO 100 with plain PPG 2000, it was observed that during the initial run, there is a small difference in the COF, but it kept increasing with time. This difference in the COF between these oils was larger with time as the test progressed. This type of phenomenon was also observed while comparing PAO 100 and PPG 2000 containing 0.025 wt.% of MWCNTs. It was also noticed that introduction of a dose of 0.025 wt.% of additive in PAO 100, COF was stable throughout the test duration. The reason is that nanolubricant at the contact region (i.e., PAO 100 containing 0.025 wt.% of MWCNTs) rearrange themselves during sliding, thereby preserving excellent lubricating property for a longer duration. In the case of PPG 2000 with 0.025 wt.% MWCNTs, the coefficient of friction continuously increased with time, and at the end of the test, it was slightly lower than that of bulk PPG 2000.

**3.3.2 Wear Performance of Nanolubricants.** Figure 5(d) and (e) demonstrates the wear volume (WV) of ball and disk specimen and percentage reduction in WV as a function of varying concentration of MWCNTs for both base oils. The wear volume was estimated as the sum of wear volume

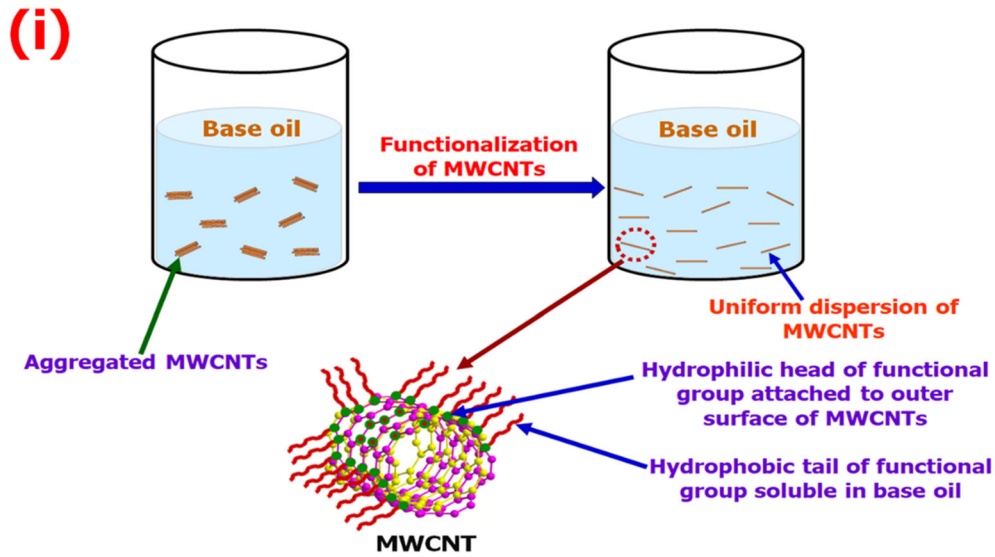
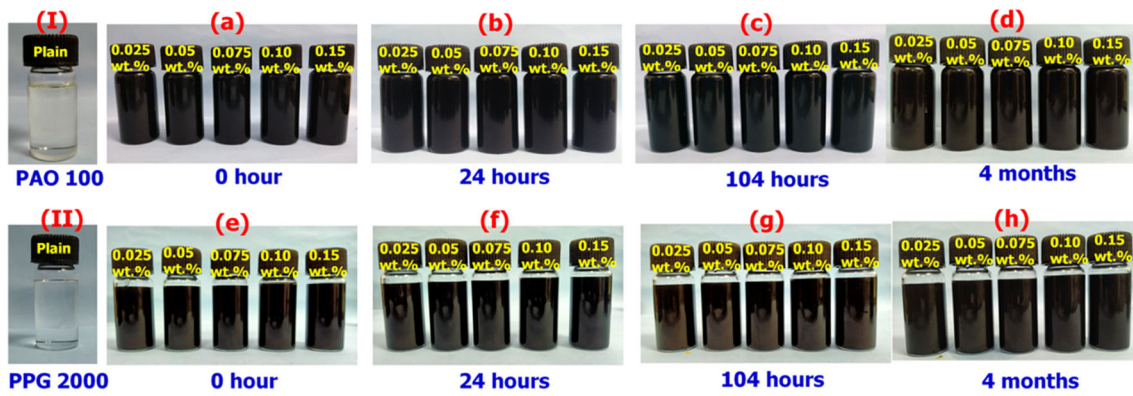


**Fig. 2** Photographs of MWCNTs suspension stability at different time intervals, (a–d) PAO 100 and (e–h) PPG 2000. (i) demonstrates the role of functional group to improve the dispersion stability in the base oils.

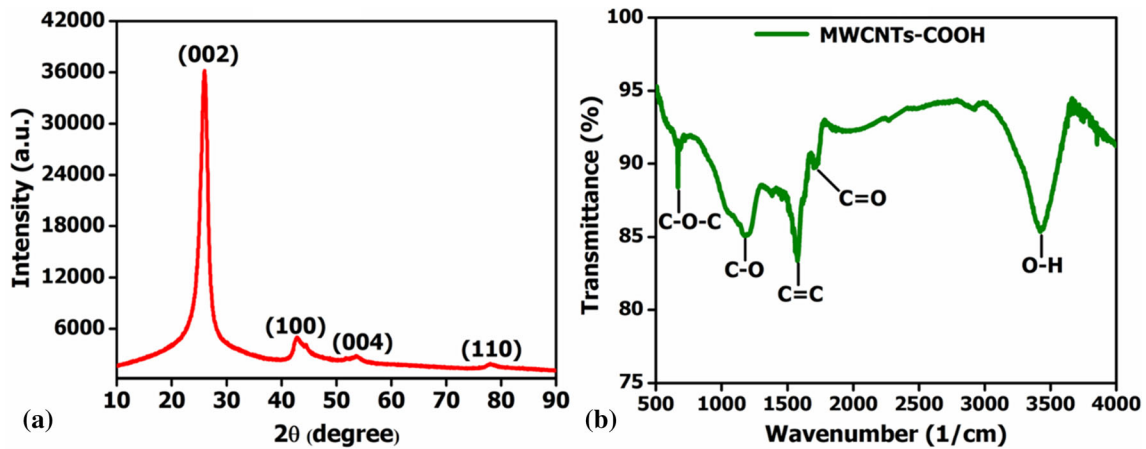


**Fig. 3** (a) XRD pattern, (b) FTIR spectrum of COOH-functionalized MWCNTs

produced in both mating surfaces. For PAO 100, the wear volume continuously decreased with an increase in the amount of additive up to 0.05 wt.%. But there was a sudden spurt in wear at a concentration of 0.075 wt.%, which was higher than that of pure PAO 100. The reason for this is that when the

quantity of additive is small (0.05 wt.%) in PAO 100, the diminutive size and tubular shape of MWCNTs have an easy entrance between the mating pairs and which easily rolls and leads to a decrease in friction as well as wear, whereas an increasing amount of nanoadditive beyond concentration 0.05

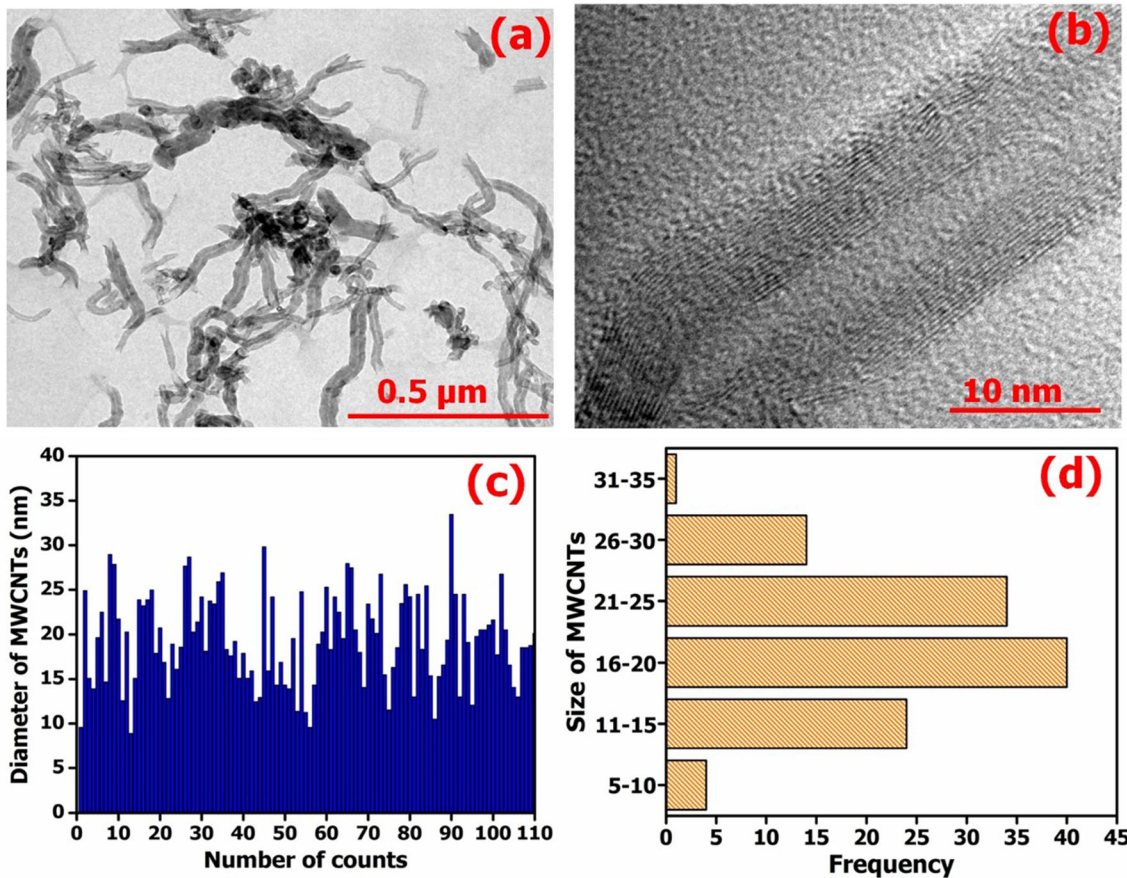


**Fig. 4** (a), (b) HR-TEM image of COOH-functionalized MWCNTs, (c) variation in the diameter of MWCNTs, (d) size and frequency distribution of additive

wt.% in PAO 100 has caused a process of fluid film build-up and collapse due to agglomeration of MWCNTs followed by the three-body abrasion, which results in diminishing the rolling capability of MWCNTs, thereby increasing the wear of the mating bodies as well as an increasing friction (Ref 46) (as displayed in Fig. 5(a)). It was concluded from Fig. 5(d) that the variation of wear volume for PPG 2000 (as projected on the secondary Y-axis) is higher as compared to PAO 100. In PAO 100, the minimum wear volume (i.e.,  $6.28 \times 10^{-3} \text{mm}^3$ ) was observed at 0.05 wt.% of MWCNTs, whereas for PPG 2000 it was observed at 0.025 wt.% of MWCNTs (i.e.,  $109.42 \times 10^{-3} \text{mm}^3$ ). The test results showed that a higher reduction in wear volume of around 87% was achieved in the case of PPG 2000 with 0.025 wt.% of MWCNTs as compared to the bulk PPG 2000. However, at all concentrations of MWCNTs in PAO 100, an excellent reduction in wear volume is observed as compared to PPG 2000-based nanolubricant.

### 3.4 Analysis of Worn Surfaces

**3.4.1 Analysis of Worn Surface of Steel Balls.** To probe the anti-wear mechanism of COOH-functionalized MWCNTs, the test balls lubricated with pure base oils and base oils containing MWCNTs were investigated using SEM and SPM and are presented in Fig. 6 and 7. The worn surface lubricated by pure PPG 2000 in Fig. 6(a) and (a<sub>1</sub>) revealed more prominent scar with deep furrows, large pits and a considerable amount of wear debris along the sliding direction. It can be

anticipated that due to continuous sliding of friction pairs, the lubricant is unable to preserve the tribo-film because the quantity of lubricant used was 0.3 ml, which leads to the occurrence of surface-originated spalling. Adhesive wear and abrasive wear are identified as the prime mode of wear. The worn surface of PPG 2000 containing concentration 0.025 wt.% of MWCNTs, presented in Fig. 6(b) and (b<sub>1</sub>), also showed a bigger wear scar but smaller than pure PPG 2000 with relatively sleek rubbing marks, which demonstrated that furrows were alleviated due to the addition of MWCNTs. However, the wear scar of steel ball lubricated with pure PAO 100 is smaller (Fig. 6(c)) as compared to the pure PPG 2000 and PPG 2000 with 0.025 wt.% of the additive. PAO 100 exhibited better characteristics (higher viscosity and higher VI) in comparison to PPG 2000, exhibiting a mixed or partial lubrication regime. In contrast, a boundary lubrication process was observed in the case of PPG 2000, as calculated using Eq 7. This mixed lubrication regime caused the separation of the mating surfaces and enhanced tribological performance. The anti-wear property of PAO 100 was further enhanced with the inclusion of 0.05 wt.% of additive, as shown in Fig. 6(d-d<sub>1</sub>). The enlarged view (at higher magnification) of wear scar for PAO 100 (Fig. 6(c<sub>1</sub>)) clearly shows the deep furrow and micropit along the direction of sliding. Further, the worn surface demonstrated the presence of MWCNTs (Fig. 6(d<sub>1</sub>)) and light furrows, which implied better friction surfaces. The aforementioned SEM results were also confirmed by the SPM

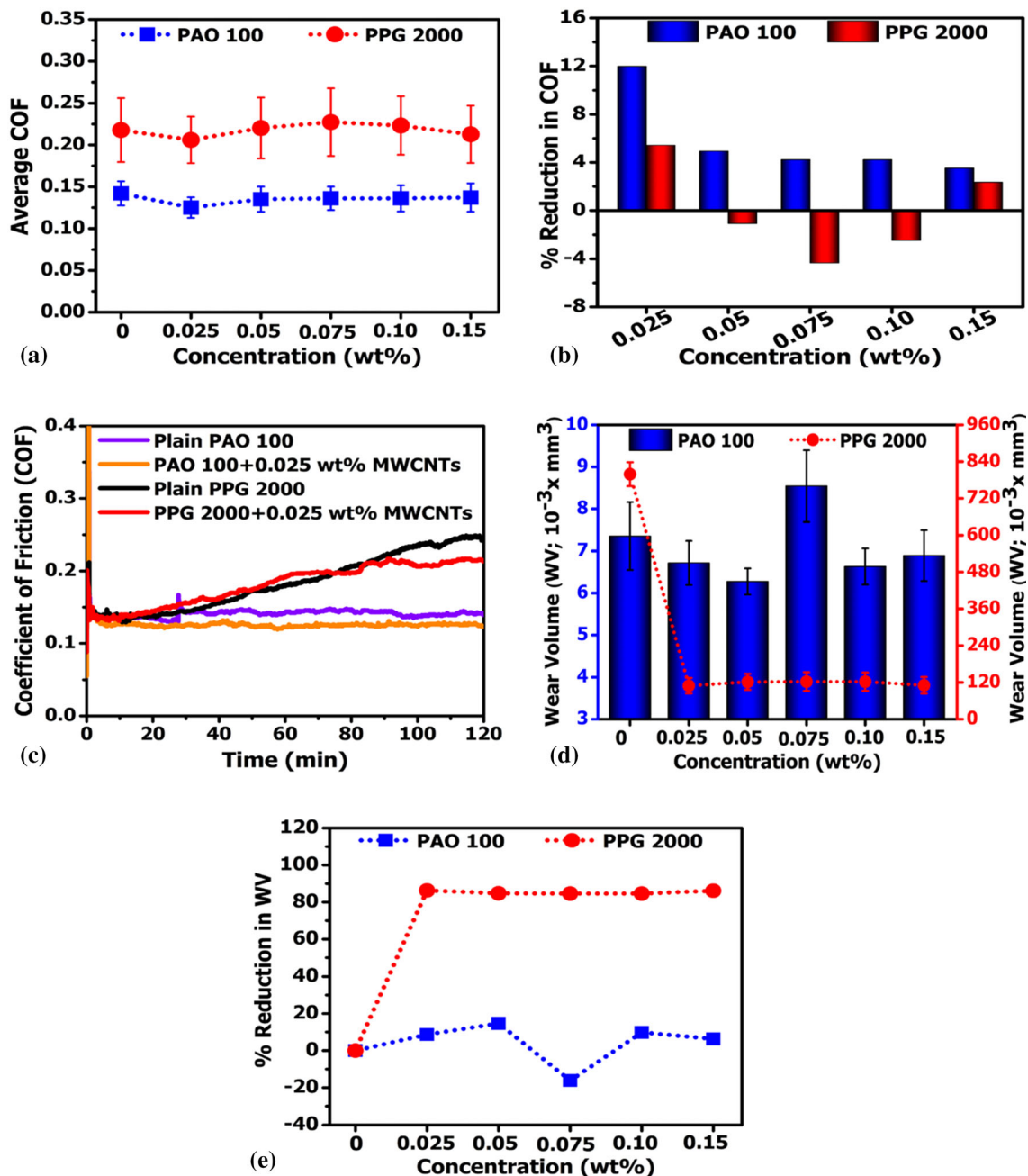


**Fig. 5** Variation of coefficient of friction (a) with different concentrations of additive in PAO 100, PPG 2000, (b) percentage reduction in COF (c) with test duration, (d) the variation of wear volume with different compositions of additive in both base oils. (e) Percentage reduction in WV

technique. The SPM images and corresponding roughness values of the worn surfaces of steel balls for different lubrication compositions are shown in Fig. 7 and Table 3. PPG 2000 (Fig. 7(a-a<sub>1</sub>)) revealed the plowing marks and deeply grooved features on the worn surface, while the less furrows and comparably smooth surface was observed when MWCNTs were added to PPG 2000 (Fig. 7(b-b<sub>1</sub>)). The height of asperity in 3D view of worn surface lubricated with PPG 2000 with 0.025 wt.% of MWCNTs is higher than that of pure PPG 2000. The peeling pit, evident in the left corner of 2 D image (Fig. 7(b)), is responsible for the increase in the height of asperity, and this type of pit is also clearly visible in Fig. 6(b). Apart from this single asperity, the worn surface seems to be

smoother. The surface roughness (Sq) of worn surface lubricated with pure PPG 2000 and pure PAO 100 are 375 and 283 nm, respectively, whereas for the scar related to 0.025 wt.% MWCNTs in PPG 2000 and 0.05 wt.% in PAO 100, the surface roughness was decreased to 305 and 225.51 nm, respectively. From the above discussion, it is apparent that incorporation of additive could improve the anti-wear response of both base oils.

**3.4.2 Worn Surface Analysis of Disk.** The counterpart (i.e., disk) of 'ball on disk' configuration of tribo-testing was also analyzed by SEM to understand the role of nanoadditive in the anti-wear performance of both types of base oils. The wear scar on the disk was also examined for width, depth and also the cross section area of the worn surface. Figure 8 shows the

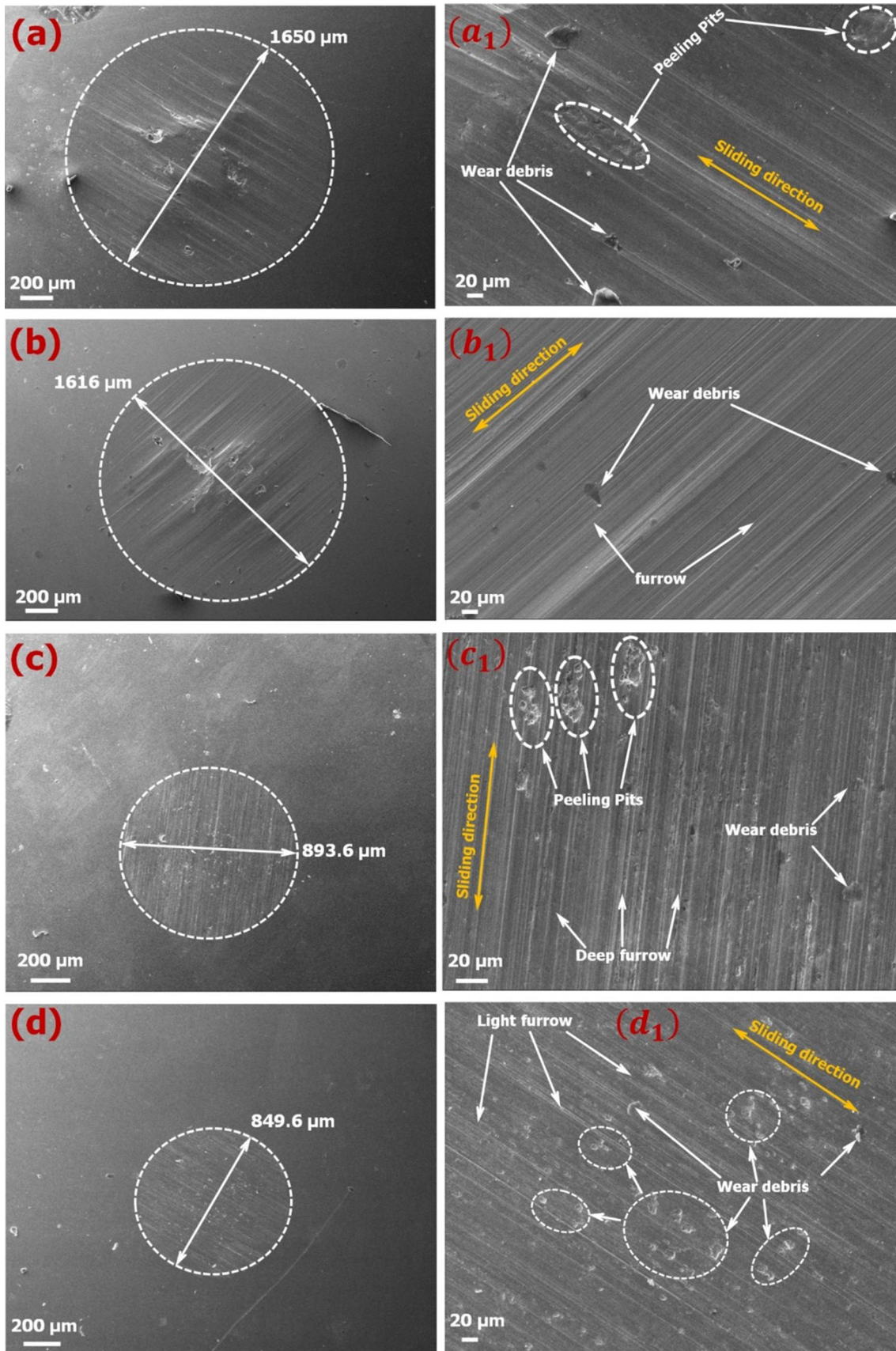


**Fig. 6** SEM micrographs of wear scars of steel balls lubricated by (a, a<sub>1</sub>) pure PPG 2000; (b, b<sub>1</sub>) PPG 2000 with 0.025 wt.% MWCNTs; (c, c<sub>1</sub>) pure PAO 100; (d, d<sub>1</sub>) PAO 100 with 0.05 wt.% MWCNTs [ Note: a, b, c, d: at 100 X; and a<sub>1</sub>, b<sub>1</sub>, c<sub>1</sub>, d<sub>1</sub>: at 1000X]



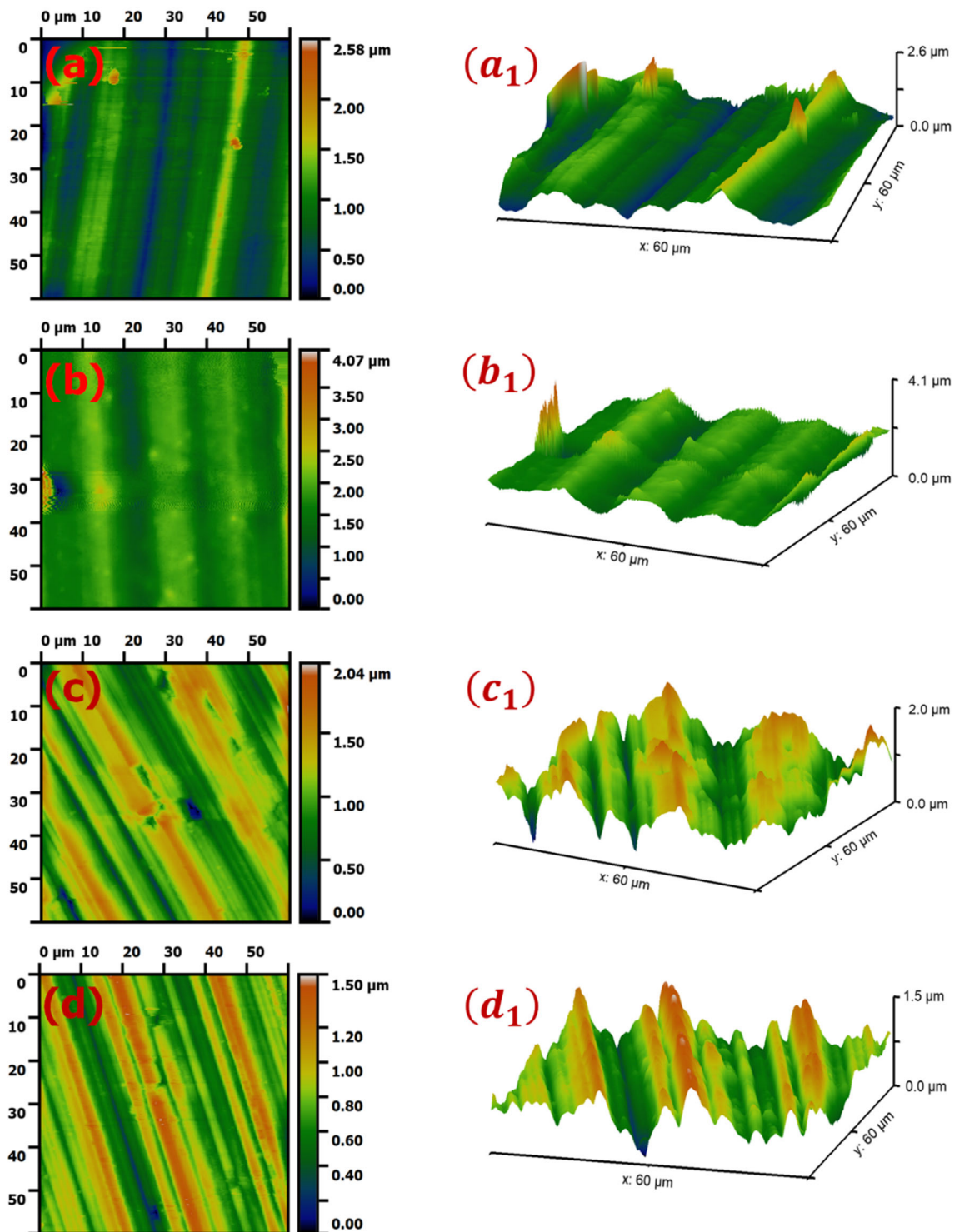


**Fig. 7** SPM pictures of worn surfaces of steel balls experimented with (a, a<sub>1</sub>) pure PPG 2000; (b, b<sub>1</sub>) PPG 2000 with 0.025 wt.% MWCNTs; (c, c<sub>1</sub>) pure PAO 100; (d, d<sub>1</sub>) PAO 100 with 0.05 wt.% MWCNTs [ Note: a, b, c, d: Top view and a<sub>1</sub>, b<sub>1</sub>, c<sub>1</sub>, d<sub>1</sub>: Three-dimensional view of worn surfaces]

SEM images of worn disk lubricated by pure base oils and base oils incorporating MWCNTs. The corresponding cross section profiles of wear track and typical values of various characteristics of worn surface are presented in Fig. 9 and Table 4,

respectively. It can be seen from Fig. 8(a-a<sub>1</sub>) that the width of the wear track on the disk lubricated by pure PPG 2000 is 1612 μm, which revealed a sign of severe scuffing. The wear surface is covered with grinding marks, a large number of furrows with

**Table 3 The summary of surface roughness of worn steel balls for various lubricant formulations**

Samples	Line roughness		Surface roughness	
	$R_a$ , nm	$R_q$ , nm	$S_a$ , nm	$S_q$ , nm
PPG 2000	236	286	293	375
PPG 2000+0.025 wt.% MWCNTs	345	447	235	305
PAO 100	206	271	232	283
PAO 100 +0.05 wt.% MWCNTs	202	245	183.78	225.51

some pits and also some amount of residual wear debris. The wear surface along the direction of movement exhibited features of adhesion, and the occurrence of plowing resulted in higher friction and wear behavior of pure PPG 2000 (Fig. 5). The depth of wear track for PPG 2000 varies between  $-3.06$  and  $-64.84$   $\mu\text{m}$  with an average depth of  $63.2$   $\mu\text{m}$  and the corresponding cross section area was  $36,136$   $\mu\text{m}^2$  (Fig. 9(a) and Table 4). It can be seen from Fig. 8(b-b<sub>1</sub>) that the wear track width decreased to  $1557$   $\mu\text{m}$  and wide furrow with the relatively smoother surface was observed when 0.025 wt% MWCNTs was added in PPG 2000. Consequently, average depth and cross section area of worn surface also decreased to  $61.8$   $\mu\text{m}$  and  $33,264$   $\mu\text{m}^2$ , respectively (Fig. 9(a) and Table 4). For pure PAO 100, the track width, average depth and cross section area of worn surface of the disk are approximately  $844.6$   $\mu\text{m}$ ,  $6.8$   $\mu\text{m}$  and  $1873$   $\mu\text{m}^2$ , respectively, as shown in Fig. 9(b) and Table 4. For 0.05 wt.% MWCNTs added in PAO 100, the track width, depth and cross section area were appreciably reduced, and their values are around  $809.8$   $\mu\text{m}$ ,  $5.2$   $\mu\text{m}$  ( $\sim 24$  % reduction) and  $1212$   $\mu\text{m}^2$  ( $\sim 36$  % reduction), respectively, which is also corroborated by SEM results of the worn disk (Fig. 8(c-d)).

**3.4.3 EDS Analysis of Worn Surfaces.** The EDS was carried out to ascertain the elemental composition and contribution of MWCNTs in the formation of tribo-film on the contacting surfaces. Figure 10 represents the EDS spectrum along with weight % and atomic % of individual elements of the selected rubbed surfaces of steel balls. The EDS results of the worn surface of the disk (Fig. 8) are summarized in Table 5. It was observed from Fig. 10 and Table 5 that the EDS spectra reveal the presence of Fe, C, Cr and O in all the worn surfaces. Fe, C and Cr are from the steel ball and disk since these are the main constituents of test specimens but the presence of C on the worn surface arises due to the concentration of MWCNTs or due to the base oil. The existence of O reveals the development of the oxide layer between the mating surface when iron is exposed to air. The surfaces lubricated by pure PPG 2000 (Fig. 10 and Table 5) displayed a higher content of oxygen among all the worn surfaces confirming the formation of an iron oxide layer. This type of oxide formation is the simplest form of the hindrance of wear, but the breakdown of these oxide layers may easily occur even at light load, which results in severe wear of friction pairs as shown in Fig. 6(a-a<sub>1</sub>) and 8(a-a<sub>1</sub>). The EDS pattern of the worn surface of the ball tested in the presence of PPG 2000 containing 0.025 wt.% of MWCNTs

(Fig. 10(b-b<sub>1</sub>)) signify that the C peak, as well as its atomic %, provides evidence for the formation of a thin tribo-film, whereas EDS spectra of worn surface of disk lubricated by pure PPG 2000 (Table 5) show the higher atomic % of C, which is due to the presence of a huge amount of wear debris on the surface (Fig. 8(a-a<sub>1</sub>)). The wear particles are also composed of iron, carbon and oxygen. The PAO 100 with 0.05 wt.% MWCNTs-lubricated surface (Fig. 10(d-d<sub>1</sub>)) has the lowest oxygen content and the highest carbon content among all tested surfaces, which imply that the polar functional group enables the adsorption of MWCNTs on the friction surface to form a lubricating film (Ref 47), which causes a low wear ( $6.274 \times 10^{-3}$   $\text{mm}^3$ ).

**3.4.4 Proposed Lubrication Mechanism.** Based on the tribological results, analysis of the worn surfaces and based on recent literature, a schematic model of lubrication mechanism for different lubricant formulations has been proposed and is presented in Fig. 11. For the surfaces lubricated with a base oil, only the oxide layer (tribo-layer) was formed between the friction pairs, which protected the surfaces up to a certain limit. However, with the progress of time and continuous tribological loading, this oxide layer breaks down, which leads to the removal of material at the interface due to metal-to-metal contact at the asperity. This phenomenon demonstrates an increase in friction and the combined action of various common wear mechanisms such as abrasive wear like microplowing and pits along with adhesion (as can be seen in Fig. 6 and 8) (Ref 48). On the contrary, when COOH-functionalized MWCNTs were mixed in a pure base oil, the polar functional group facilitates the MWCNTs to be adsorbed on the friction surface to form a protective lubricating film, which separates the mating surface, thereby decreasing friction and wear. The high thermal conductivity of MWCNTs also enables resistance to friction heat, lowering the surface temperature and minimizing the probability of adhesion between the rubbing surfaces. It also ameliorates the lubricating effect owing to a unique hexagonal structure (Ref 49). The MWCNTs easily enter into groves and openings of the rubbing surfaces; therefore, pressure can be disseminated over a large contact area, validating the mending effect. Furthermore, it is also presumed that the rolling effect of MWCNTs is prevailing throughout the entire friction process because of good ingrained stability of the additive between the mating surfaces. It may also be speculated that at a higher load, MWCNTs can be decorticated (exfoliated) into a lamellar shape (i.e., nanosheets of graphene), which deterior-

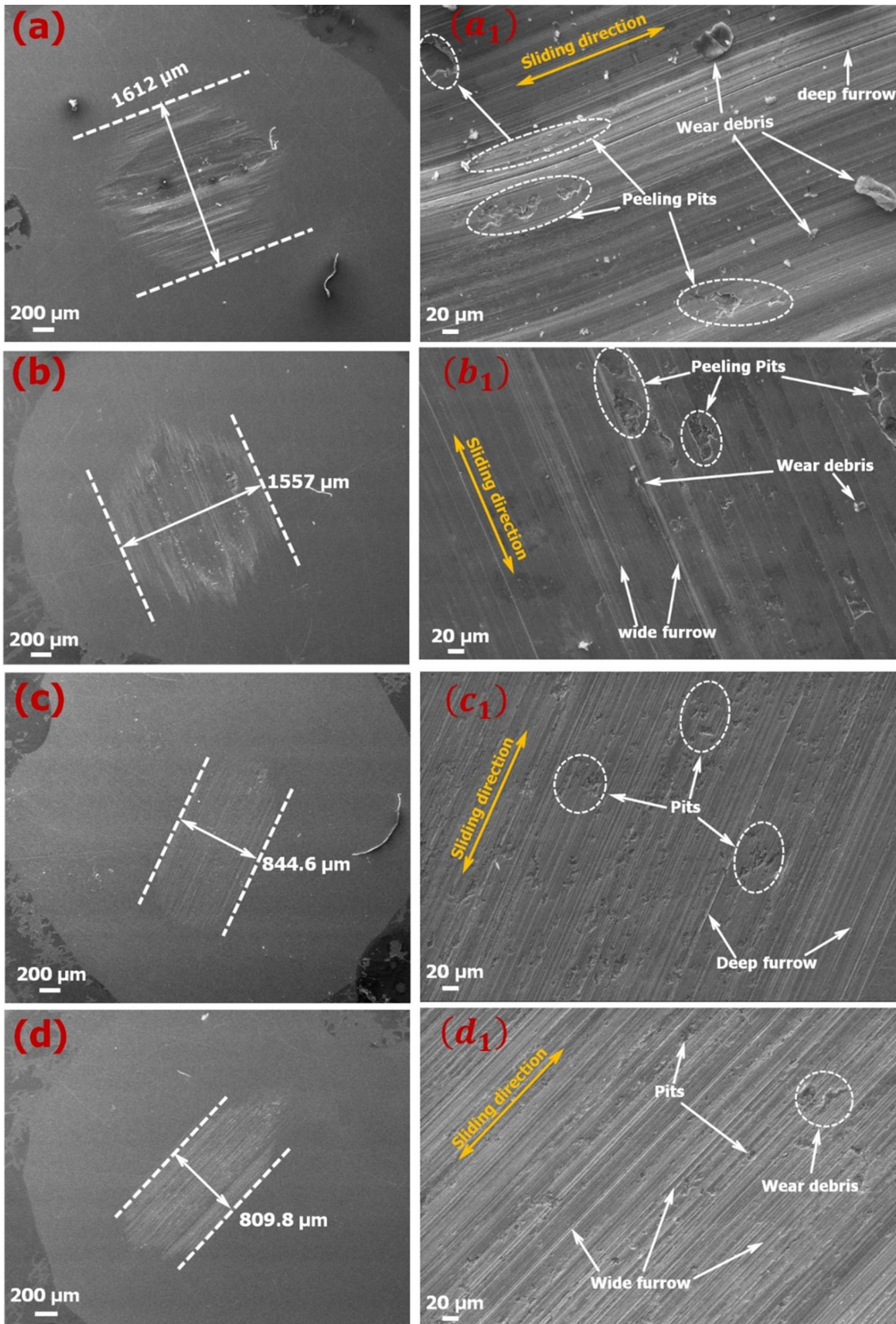


**Fig. 8** SEM images of wear scar of the steel disk after friction test (a, a<sub>1</sub>) pure PPG 2000; (b, b<sub>1</sub>) PPG 2000 with 0.025 wt.% MWCNTs; (c, c<sub>1</sub>) pure PAO 100; (d, d<sub>1</sub>) PAO 100 with 0.05 wt.% MWCNTs [ Note: a, b, c, d: at 100 X; and a<sub>1</sub>, b<sub>1</sub>, c<sub>1</sub>, d<sub>1</sub>: at 500X]

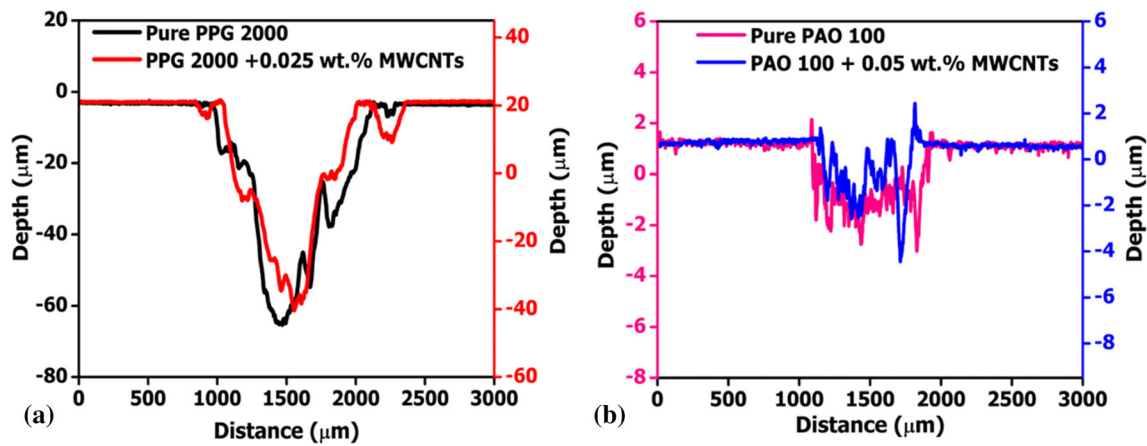


**Fig. 9** The cross section profile of wear track of the disk lubricated with (a) pure PPG 2000 and PPG 2000 with 0.025 wt.% MWCNTs, (b) pure PAO 100 and PAO 100 with 0.05 wt.% MWCNTs

**Table 4** The summary of the various characteristics of worn steel disk for different lubricants

Samples	Wear track width, $\mu\text{m}$	Wear track depth, $\mu\text{m}$	Cross section area, $\mu\text{m}^2$
PPG 2000	1612	63.2	36136
PPG 2000+0.025 wt.% MWCNTs	1557	61.8	33264
PAO 100	844.6	6.8	1873
PAO 100 +0.05 wt.% MWCNTs	809.8	5.2	1212

rated the rolling motion of MWCNTs, thereby increasing the COF (as evident in case of PAO 100 with 0.05 wt.%) (Ref 50-52). Nevertheless, these nanosheets stick to the surfaces and act as a solid lubricant, which contributes to the formation of transfer layer at the interface of rubbing surfaces, thereby significantly diminishing the wear (Figure 5). The adhesion of these fragments may affect the surfaces of worn surfaces in terms of either degradation or comparable enhancement (Ref 47). In this study, the worn surfaces lubricated with MWCNTs-based nanolubricants were relatively polished in comparison to the worn surfaces tested with pure base oils, as evident by SEM and SPM analyses.

#### 4. Conclusions

The following conclusions have been drawn from the present investigation.

- COOH-functionalized MWCNTs at different compositions (i.e., 0.025, 0.05, 0.075, 0.1, 0.15 wt%) were dispersed in two types of base oil (i.e., PAO 100 and PPG 2000). The tribological performance of both the base oils improved

with the addition of MWCNTs as an additive. Overall, PAO 100 exhibited better tribological performance as compared to PPG 2000.

- The test results showed that maximum reduction in wear volume of around 87% was achieved in the case of PPG 2000 containing 0.025 wt.% of additive as compared to pure PPG 2000. However, PAO 100 at all concentrations of MWCNTs showed lower wear volume as compared to PPG 2000-based nanolubricant. PAO 100 with 0.05 wt.% of additive offered the maximum reduction in the wear volume (~ 15%).
- The introduction of 0.025 wt.% dose of MWCNTs in both oils exhibited maximum reduction in friction coefficient. The test results revealed that PAO 100-based nanolubricants displayed the lowest friction coefficient as compared to PPG 2000-based nanolubricants.
- The enhanced tribological performances of both base oils are attributed to good dispersion consistency of MWCNTs in the base oils and ingrained embedded stability of the additive between the mating surfaces, generation of nanolubrication effects such as rolling, mending, polishing effect and also the formation of surface-protective tribo-film at the mating surface.

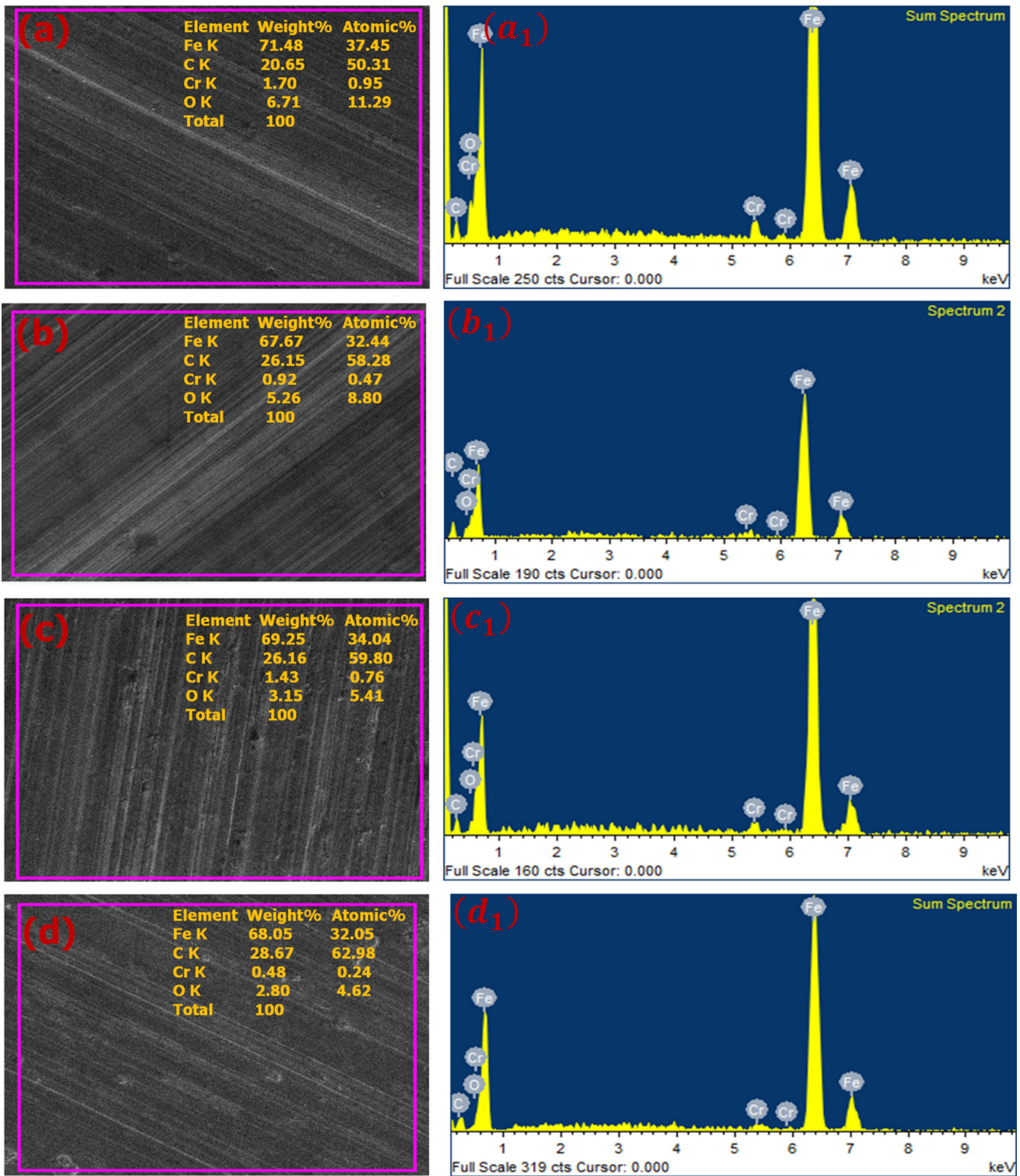


**Fig. 10** EDS spectra of wear scars of steel balls tested with (a, a<sub>1</sub>) pure PPG 2000; (b, b<sub>1</sub>) PPG 2000 with 0.025 wt.% MWCNTs; (c, c<sub>1</sub>) pure PAO 100; (d, d<sub>1</sub>) PAO 100 with 0.05 wt.% MWCNTs

**Table 5** The summary of typical values of elements presented on the worn surfaces of disk lubricated with different oil compositions

Lubricant composition	Weight %				Atomic %			
	Fe	C	Cr	O	Fe	C	Cr	O
Pure PPG 2000	61.46	29.06	1.06	8.43	27.06	59.49	0.50	12.95
PPG 2000+0.025 wt.% MWCNTs	76.46	21.19	1.54	1.63	42.21	54.40	0.91	2.65
Pure PAO 100	72.72	22.56	0.84	3.87	37.86	54.63	0.47	7.04
PAO 100 +0.05 wt.% MWCNTs	73.45	22.02	0.76	3.77	38.70	53.94	0.43	6.49

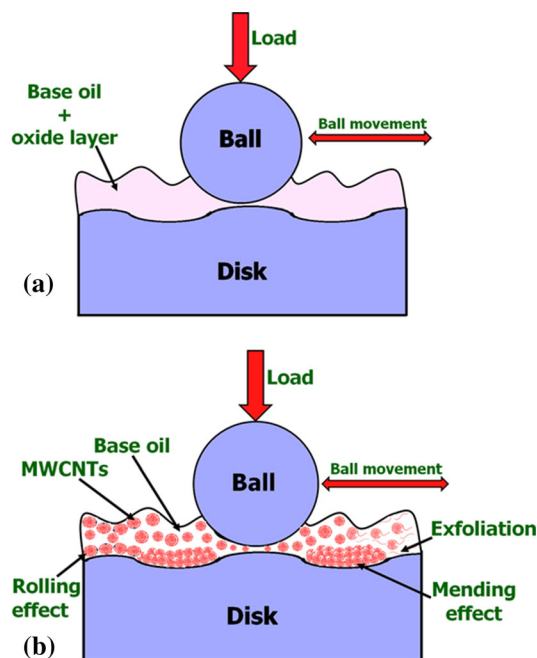


**Fig. 11** Lubrication mechanisms with (a) pure base oil, (b) base oil containing MWCNTs

### Acknowledgments

The authors are thankful to the Central Instrument Facility (CIF), IIT (BHU) for the characterization of the samples. One of the authors (A.P. Harsha) would like to thank the staff of the fretting wear group, 6.3 Division of Macro Tribology and Wear Protection, Federal Institute for Materials Research and Testing (BAM), Berlin, Germany, for their support during the experimental studies. We also thank BAM for providing financial support for the duration of this research during the stay for the work.

### References

1. S. Iijima, Helical Microtubules of Graphitic Carbon, *Nature*, 1991, **354**, p 56–58
2. S. Mallakpour and S. Soltanian, Surface Functionalization of Carbon Nanotubes: Fabrication and Applications, *RSC Adv.*, Royal Society of Chemistry, 2016, **6**(111), p 109916–109935
3. S. Shahnazar, S. Bagheri, and S.B. Abd Hamid, Enhancing Lubricant Properties by Nanoparticle Additives, *Int. J. Hydrogen Energy*, Elsevier Ltd, 2016, **41**(4), p 3153–3170
4. J.H. Lehman, M. Terrones, E. Mansfield, K.E. Hurst, and V. Meunier, Evaluating the Characteristics of Multiwall Carbon Nanotubes, *Carbon N. Y.*, Elsevier Ltd, 2011, **49**(8), p 2581–2602

5. Y. Peng and Z. Ni, Tribological Properties of Stearic Acid Modified Multi-Walled Carbon Nanotubes in Water, *J. Tribol.*, 2013, **135**(1), p 1–5
6. D. Tasis, N. Tagmatarchis, A. Bianco and M. Prato, Chemistry of Carbon Nanotubes, *Chem. Rev.*, 2006, **106**(3), p 1105–1136
7. X. Pei, L. Hu, W. Liu and J. Hao, Synthesis of Water-Soluble Carbon Nanotubes via Surface Initiated Redox Polymerization and Their Tribological Properties as Water-Based Lubricant Additive, *Eur. Polym. J.*, 2008, **44**(8), p 2458–2464
8. C.S. Chen, X.H. Chen, L.S. Xu, Z. Yang and W.H. Li, Modification of Multi-Walled Carbon Nanotubes with Fatty Acid and Their Tribological Properties as Lubricant Additive, *Carbon N. Y.*, 2005, **43**(8), p 1660–1666
9. F.H. Gojny, J. Nastalczyk, Z. Roslaniec and K. Schulte, Surface Modified Multi-Walled Carbon Nanotubes in CNT/Epoxy-Composites, *Chem. Phys. Lett.*, 2003, **370**(5-6), p 820–824
10. Y. Choi, J. and Zhang, "Single, Double, MultiWall Carbon Nanotube Properties & Applications," *Aldrich Materials Science, Sigma-Aldrich Co. LLC.*, 2018
11. W. Khalil, A. Mohamed, M. Bayoumi and T.A. Osman, Tribological Properties of Dispersed Carbon Nanotubes in Lubricant, *Fullerenes Nanotub. Carbon Nanostructures*, 2016, **24**(7), p 479–485
12. S.M. Muzakir, K.P. Lijesh and H. Hirani, Influence of Surfactants on Tribological Behaviors of MWCNTs (Multi-Walled Carbon Nanotubes), *Tribol. - Mater. Surfaces Interfaces*, 2016, **10**(2), p 74–81
13. V. Chauveau, D. Mazuyer, F. Dassenoy and J. Cayer-Barrioz, In Situ Film-Forming and Friction-Reduction Mechanisms for Carbon-Nanotube Dispersions in Lubrication, *Tribol. Lett.*, 2012, **47**(3), p 467–480
14. B. Wang, W. Tang, X. Liu, and Z. Huang, Synthesis of Ionic Liquid Decorated Multi-Walled Carbon Nanotubes as the Favorable Water-Based Lubricant Additives, *Appl. Phys. A Mater. Sci. Process.*, Springer Berlin Heidelberg, 2017, **123**(11), p 680
15. B. Yu, Z. Liu, C. Ma, J. Sun, W. Liu and F. Zhou, Ionic Liquid Modified Multi-Walled Carbon Nanotubes as Lubricant Additive, *Tribol. Int.*, 2015, **81**(January), p 38–42
16. B. Yu, Z. Liu, F. Zhou, W. Liu and Y. Liang, A Novel Lubricant Additive Based on Carbon Nanotubes for Ionic Liquids, *Mater. Lett.*, 2008, **62**(17-18), p 2967–2969
17. Y. Peng, Y. Hu and H. Wang, Tribological Behaviors of Surfactant-Functionalized Carbon Nanotubes as Lubricant Additive in Water, *Tribol. Lett.*, 2007, **25**(3), p 247–253
18. R. Benda, J. Bullen and A. Plomer, Synthetic Basics: Polyalphaolefins - Base Fluids for High-Performance Lubricants, *J. Synth. Lubr.*, 1996, **13**(1), p 40–57
19. L.R. Rudnick, in *Synthetics, Mineral Oils, and Bio-Based Lubricants: Chemistry and Technology*, L.R. Rudnick, Ed., (New York, NY), CRC Press, 2005
20. G. Yang, J. Zhang, S. Zhang, L. Yu, P. Zhang, and B. Zhu, Preparation of Triazine Derivatives and Evaluation of Their Tribological Properties as Lubricant Additives in Poly-Alpha Olefin, *Tribol. Int.*, Elsevier, 2013, **62**, p 163–170
21. R. Chou, A.H. Battez, J.J. Cabello, J.L. Viesca, A. Osorio and A. Sagastume, Tribological Behavior of Polyalphaolefin with the Addition of Nickel Nanoparticles, *Tribol. Int.*, 2010, **43**(12), p 2327–2332
22. S. Paskvale, M. Remškar and M. Čekada, Tribological Performance of TiN, TiAlN and CrN Hard Coatings Lubricated by MoS<sub>2</sub> Nanotubes in Polyalphaolefin Oil, *Wear*, 2016, **352-353**, p 72–78

23. N.G. Demas, E. V. Timofeeva, J.L. Routbort, and G.R. Fenske, Tribological Effects of BN and MoS<sub>2</sub> Nanoparticles Added to Polyalphaolefin Oil in Piston Skirt/Cylinder Liner Tests, *Tribol. Lett.*, American Society of Mechanical Engineers, 2012, **47**(1), p 91–102
24. S.M. Alves, V.S. Mello, E.A. Faria, and A.P.P. Camargo, Nanolubricants Developed from Tiny CuO Nanoparticles, *Tribol. Int.*, Elsevier, 2016, **100**, p 263–271
25. M. Zhang, X. Wang, X. Fu and Y. Xia, Performance and Anti-Wear Mechanism of CaCO<sub>3</sub> Nanoparticles as a Green Additive in Poly-Alpha-Olefin, *Tribol. Int.*, 2009, **42**(7), p 1029–1039
26. J.L. Viesca, A. Hernández Battez, R. González, R. Chou, and J.J. Cabello, Antiwear Properties of Carbon-Coated Copper Nanoparticles Used as an Additive to a Polyalphaolefin, *Tribol. Int.*, 2011, **44**(7-8), p 829–833
27. M. Zhang, X. Wang and W. Liu, Tribological Behavior of LaF<sub>3</sub> Nanoparticles as Additives in Poly-alpha-olefin, *Ind. Lubr. Tribol.*, 2013, **65**(4), p 226–235
28. T. Zolper, Z. Li, C. Chen, M. Jungk, T. Marks, Y.-W. Chung and Q. Wang, Lubrication Properties of Polyalphaolefin and Polysiloxane Lubricants: Molecular Structure-Tribology Relationships, *Tribol. Lett.*, 2012, **48**(3), p 355–365
29. K. Li, X. Zhang, C. Du, J. Yang, B. Wu, Z. Guo, C. Dong, N. Lin and C. Yuan, Friction Reduction and Viscosity Modification of Cellulose Nanocrystals as Biolubricant Additives in Polyalphaolefin Oil, *Carbohydr. Polym.*, 2019, **220**, p 228–235
30. W. Yue, X. Sun, C. Wang, Z. Fu, Y. Liu, and J. Liu, A Comparative Study on the Tribological Behaviors of Nitrided and Sulfur-Nitrided 35CrMo Steel Lubricated in PAO Base Oil with MoDTC Additive, *Tribol. Int.*, Elsevier, 2011, **44**(12), p 2029–2034
31. J. Kogovšek and M. Kalin, Various MoS<sub>2</sub>-, WS<sub>2</sub>- and C-Based Micro- and Nanoparticles in Boundary Lubrication, *Tribol. Lett.*, 2014, **53**(3), p 585–597
32. N. Nunn, Z. Mahbooba, M.G. Ivanov, D.M. Ivanov, D.W. Brenner and O. Shenderova, Tribological Properties of Polyalphaolefin Oil Modified with Nanocarbon Additives, *Diam. Relat. Mater.*, 2015, **54**(April), p 97–102
33. D. Beatty and M. Greaves, Polyalkylene Glycol Synthetic PAG Oil Explained, *Mach. Lubr. Mag.*, 2006, **9**(September), p 1–7, <https://www.machinerylubrication.com/Read/930/pag-synthetic-oil>
34. The Dow Chemical Company, “Product Safety Assessment Polyglycol P Series Polymers, FLUENT Brand Polyglycol,” The Dow Chemical Company, 2014, p 1–6
35. M.R. Greaves, Polyalkylene Glycols: Present and Future Applications, *Tribol. Lubr. Technol.*, 2013, **69**(6), p 34–39
36. S. Igari, S. Mori and Y. Takikawa, Effects of Molecular Structure of Aliphatic Diols and Polyalkylene Glycol as Lubricants on the Wear of Aluminum, *Wear*, 2000, **244**(1-2), p 180–184
37. H. Xiao, S. Liu, Y. Chen, D. Han, and D. Wang, Impacts of Polypropylene Glycol (PPG) Additive and PH on Tribological Properties of Water-Based Drilling Mud for Steel-Steel Contact, *Tribol. Int.*, Elsevier Ltd, 2017, **110**(February), p 318–325
38. C. Zhang, J. Liu, C. Zhang and S. Liu, Friction Reducing and Anti-Wear Property of Metallic Friction Pairs under Lubrication of Aqueous Solutions with Polyether Added, *Wear, Elsevier*, 2012, **292-293**, p 11–16
39. D. Klaffke, Fretting Wear of Ceramics, *Tribol. Int.*, 1989, **22**(2), p 89–101
40. D. Hamrock, B.J. and Dowson, “Minimum Film Thickness in Elliptical Contacts for Different Regimes of Fluid-Film Lubrication,” *NASA Technical Paper-1342*, (Cleveland, Ohio), 1978
41. W.R. Jones, R.L. Johnson, W.O. Winer, and D.M. Sanborn, Pressure-Viscosity Measurements for Several Lubricants to  $5.5 \times 10^8$  Newtons Per Square Meter ( $8 \times 10^4$  PSI) and 149 C (300 F), *A S L E Trans.*, 1975, **18**(4), p 249–262
42. B.J. Hamrock, Schmid S. R., and B.O. Jacobson, *Fundamental of Fluid Film Lubrication*, Marcel Dekker, Inc., New York, 2004
43. V.T. Le, C.L. Ngo, Q.T. Le, T.T. Ngo, D.N. Nguyen, and M.T. Vu, Surface Modification and Functionalization of Carbon Nanotube with Some Organic Compounds, *Adv. Nat. Sci. Nanosci. Nanotechnol.*, 2013, **4**(3), p 035017
44. N.M. Vesali, A.A. Khodadadi, Y. Mortazavi, A.O. Sahraei, F. Pourfayaz and M.S. Sedghi, Functionalization of Carbon Nanotubes Using Nitric Acid Oxidation and DBD Plasma, *World Acad. Sci. Eng. Technol.*, 2009, **37**(January), p 177–179
45. V.M. Rao, C.H. Castano, J. Rojas, and A.J. Abdulghani, Synthesis of Nickel Nanoparticles on Multi-Walled Carbon Nanotubes by Gamma Irradiation, *Radiat. Phys. Chem.*, Elsevier, 2013, **89**(August), p 51–56
46. H. Kumar and A.P. Harsha, Investigation on Friction, Anti-Wear, and Extreme Pressure Properties of Different Grades of Polyalphaolefins With Functionalized Multi-Walled Carbon Nanotubes as an Additive, *J. Tribol.*, 2020, **142**(8), p 1702–1714
47. M.Y. Cheah, H.C. Ong, N.W.M. Zulkifli, H.H. Masjuki, and A. Salleh, Physicochemical and Tribological Properties of Microalgae Oil as Biolubricant for Hydrogen-Powered Engine, *Int. J. Hydrogen Energy*, Elsevier Ltd, 2020, **45**(42), p 22364–22381
48. R. Wäsche, M. Hartelt, and V.-D. Hodoroaba, Analysis of Nanoscale Wear Particles from Lubricated Steel–Steel Contacts, *Tribol. Lett.*, 2015, **58**(3), p 49
49. L. Hongtao, J. Hongmin, H. Haiping and H. Younes, Tribological Properties of Carbon Nanotube Grease, *Ind. Lubr. Tribol.*, 2014, **66**(5), p 579–583
50. J.A.C. Cornelio, P.A. Cuervo, L.M. Hoyos-Palacio, J. Lara-Romero, and A. Toro, Tribological Properties of Carbon Nanotubes as Lubricant Additive in Oil and Water for a Wheel–Rail System, *J. Mater. Res. Technol.*, Korea Institute of Oriental Medicine, 2016, **5**(1), p 68–76
51. L. Zhang, J. Pu, L. Wang and Q. Xue, Synergistic Effect of Hybrid Carbon Nanotube-Graphene Oxide as Nanoadditive Enhancing the Frictional Properties of Ionic Liquids in High Vacuum, *ACS Appl. Mater. Interfaces*, 2015, **7**(16), p 8592–8600
52. L. Zhang, J. Pu, L. Wang, and Q. Xue, Frictional Dependence of Graphene and Carbon Nanotube in Diamond-like Carbon/Ionic Liquids Hybrid Films in Vacuum, *Carbon N. Y.*, Elsevier Ltd, 2014, **80**(1), p 734–745

**Publisher's Note** Springer Nature remains neutral with regard to jurisdictional claims in published maps and institutional affiliations.